

Using stream sediment data to determine geochemical anomalies by statistical analysis and fractal modeling in Tafrash Region, Central Iran

Feridon Ghadimi^{1*}, Mohammad Ghomi^{1,2}, Ehasan Malaki¹

¹ Department of Mining Engineering, Arak University of Technology, Arak, Iran

² Department of Mining and Metallurgical Engineering, Amirkabir University of Technology, Tehran, Iran

*Corresponding author, e-mail: drghadimi@yahoo.com

(received: 07/11/2015 ; accepted: 29/02/2016)

Abstract

Iranian Cenozoic magmatic belt, known as Urumieh-Dokhtar, is recognized as an important polymetallic mineralization which hosts porphyry, epithermal, and polymetallic skarn deposits. In this regard, multivariate analyses are generally used to extract significant anomalous geochemical signature of the mineral deposits. In this study, stepwise factor analysis, cluster analysis, and concentration–area fractal model have been used to delineate geochemical anomalies associated with skarn mineralization, based on Au, Cu, Pb, Zn, Ag, Mo, W, Sn, and As stream sediment data. These results indicate that the Urumieh-Dokhtar belt potentially hosts Au skarn deposits. The hybrid method combining the statistical analysis and C-A fractal model is an effective tool to identify geochemical anomalies.

Keywords: Au Skarn Deposit, Concentration Area Fractal Model, Iran, Statistical Analysis, Stream Sediment

Introduction

Iranian Cenozoic magmatic belt, known as Urumieh-Dokhtar belt, is an interesting area for porphyry and related types of mineral resources. This belt is becoming a world-class Cu polymetallic province. Porphyry type, skarn, hydrothermal veins, hot spring type, and magmatic deposits of Cu, Pb, Zn, Au, and other metallic and non-metallic elements widely occur in this belt (Shahabpour, 1994). The porphyry-type deposits are one of the most important deposits in the Urumieh-Dokhtar belt. Skarn deposits, another important type in this belt, are exemplified by Pb, Ag, Sn deposits. Integration of stream sediment, geochemical data with other types of mineral exploration data is a challenging issue that needs careful analysis of multi-element geochemical anomalies. Analysis of stream sediment samples can reveal various geochemical anomalies, some of which can be considered as surficial geochemical signature of some type of mineralization (Zheng *et al.*, 2014).

Univariate data analyses such as histogram, box plots, density plot, and Q–Q plot, multivariate data analysis (e.g., factor analysis, cluster analysis), and fractal and multifractal models using Geographic Information System (GIS) techniques have been successfully applied to analyze geochemical data (Zuo *et al.*, 2009a, 2009b; Carranza, 2009, 2010; Grunsky, 2010; Cheng *et al.*, 2011; Arias *et al.*, 2012; Zuo, 2014; Yousefi and Nykänen, 2015). Multivariate analyses are especially useful for that

purpose because the relative importance of the combinations of geochemical variables can be evaluated. There are many studies that have used multivariate methods for analysis of geochemical exploration data (Grunsky *et al.*, 2009).

Factor analysis, as one of the methods of multivariate analysis, has been widely used for interpretation of stream sediment geochemical data (Sun *et al.*, 2009; Yousefi *et al.*, 2012, 2013). The principal aim of factor analysis is to explain the variations in a multivariate data set by as few factors as possible and to detect hidden multivariate data structures (Johnson and Wichern, 2002). Thus, factor analysis is suitable for analysis of the variability inherent in a geochemical data set with many analyzed elements. Consequently, the factor analysis is often applied as a tool for exploratory data analysis. Univariate/ multivariate data analyses based on the frequency distributions or correlations of geochemical data may be effective for solving some problems in the frequency domain but are of limited use in the spatial domain due to spatial autocorrelation inherent in geochemical data.

The fractal/ multifractal models (Cheng *et al.*, 1994; Afzal *et al.*, 2011, 2013, 2014; Heidari *et al.*, 2013; Geranian *et al.*, 2013; Yousefi & Carranza, 2015) involve both the frequency distributions and the spatial self-similar properties of geochemical variables, and have been demonstrated to be effective tools for decomposing complex and mixed geochemical populations and to identify weak

geochemical anomalies hidden within strong geochemical background (Cheng, 2007; Zuo and Xia, 2009; Cheng and Agterberg, 2009; Cheng *et al.*, 2010; Zuo, 2011a; Arias *et al.*, 2012).

In this paper, the hybrid method consisted of factor and cluster analysis and concentration-area fractal model are used to identify geochemical anomalies associated with Au skarn mineralization based on stream sediment geochemical data from the Zaghar region in the Markazi province, central Iran. Geochemical analyses of 109 stream sediment samples for Au, Cu, Pb, Zn, Ag, Mo, W, Sn, and As collected by the Geological Survey of Iran (GSI) have been used to test the proposed approach using the factor score (FS) and geochemical mineralization probability index (GMPI). In all geochemical data distribution maps described in this paper, the cumulative percentile equivalent to 97.5% frequency has been considered as a reference value/threshold to evaluate and compare the efficiency of the methods discussed in this research.

Geological Setting

The Zaghar area, of about 34.15 km², is situated about 5 km SW of Tafrash, Central Iran. This area is located in the main Iranian Cenozoic magmatic belt, known as Urumieh-Dokhtar, which is one of the subdivisions of Zagros orogenies (Alavi, 1994). This unit extends from NW to SE Iran and hosts Iranian large porphyry deposits (Shahabpour, 1994). The current configuration of geological structures of the area was developed during the Mesozoic and Cenozoic. The mineral belt also coincides with an elevated magnetic field produced by the Cenozoic intermediate intrusions (Shahabpour, 1994).

The stratigraphic sequence of the Urumieh-Dokhtar belt in the study area consists of major units. These are: (1) Triassic Formation composed of limestone in lower, sandstone and shale in upper Triassic sequence; (2) Jurassic Formation, consisted of black sandstone and shale; (3) Cretaceous sedimentary rocks consisted of limestone, marl, and sandy limestone; and (4) Eocene clastic and pyroclastic rocks composed of trachyandesitic lava, limestone, and acidic tuff (Fig. 1). Brecciated limestone of the Cretaceous Formation is the most important host rock for the Au deposit which is overlain by Eocene Formation.

The complex, superimposed regional structures in this belt include multiple deformational events and regional scale faults, such as the NW-SE

trending faults that controlled the distribution of intermediate intrusions and associated mineralization (Fig. 1). Magmatic rocks mostly intruded after the Eocene period are widespread in the region (Hajian, 1999). The Zaghar intrusion is consisted of diorite, quartz-diorite, and related hornfels. Most Au deposit of the Zaghar mineral area is spatially associated with these intermediate intrusive bodies. The Zaghar mineralized intrusion includes ore bearing stock and several dykes (Hajian, 1999).

One type of Au skarn deposit is recognized in the Zaghar mineral area. Almost a deposit of economic interest is concentrated within and around the northern margins of the Zaghar intrusion and close to Zaghar fault. The extent of metasomatic rocks and alteration intensity within and around the Zaghar intrusion is large and extensive. Skarn is the main type of ore deposit in the Zaghar mineral area. Deposit and occurrence is located within the contact zones between the dioritic intrusions and the Cretaceous limestone Formation. The skarn ore body at the contact zone between dioritic intrusion and the carbonate country rocks are composed of hematite, chalcopyrite, pyrite, galena, garnet, chlorite, epidote, quartz, and calcite. Many of these deposits show spatial zoning.

Garnet and hematite-bearing exoskarns typically occur in an external zone associated with marbles. Epidote-bearing endoskarn and altered diorite-type ores occur within diorite. Wall-rock alteration is well developed around the ore body and consists of garnet, albite, chlorite, quartz, carbonates, kaolinite, and sericite. Ore minerals of the quartz-sulphide are chalcopyrite, pyrite, and minor amounts of galena and native gold (Borna, 2004).

Materials and Methods

Stream sediments and sample collection

One of the most commonly used geochemical exploration methods of prospecting is based on the study of active stream sediments.

According to the definition given by the Forum of the European Geological Surveys (FOREGS), these are represented by the fine and medium size fraction of sediments carried and settled by second order streams (Salminen *et al.*, 1998). Stream sediments can be considered as averagely representative of the outcropping rocks in the drainage basin, upstream of the sampling point (Lahermo *et al.*, 1996: Fig. 2).

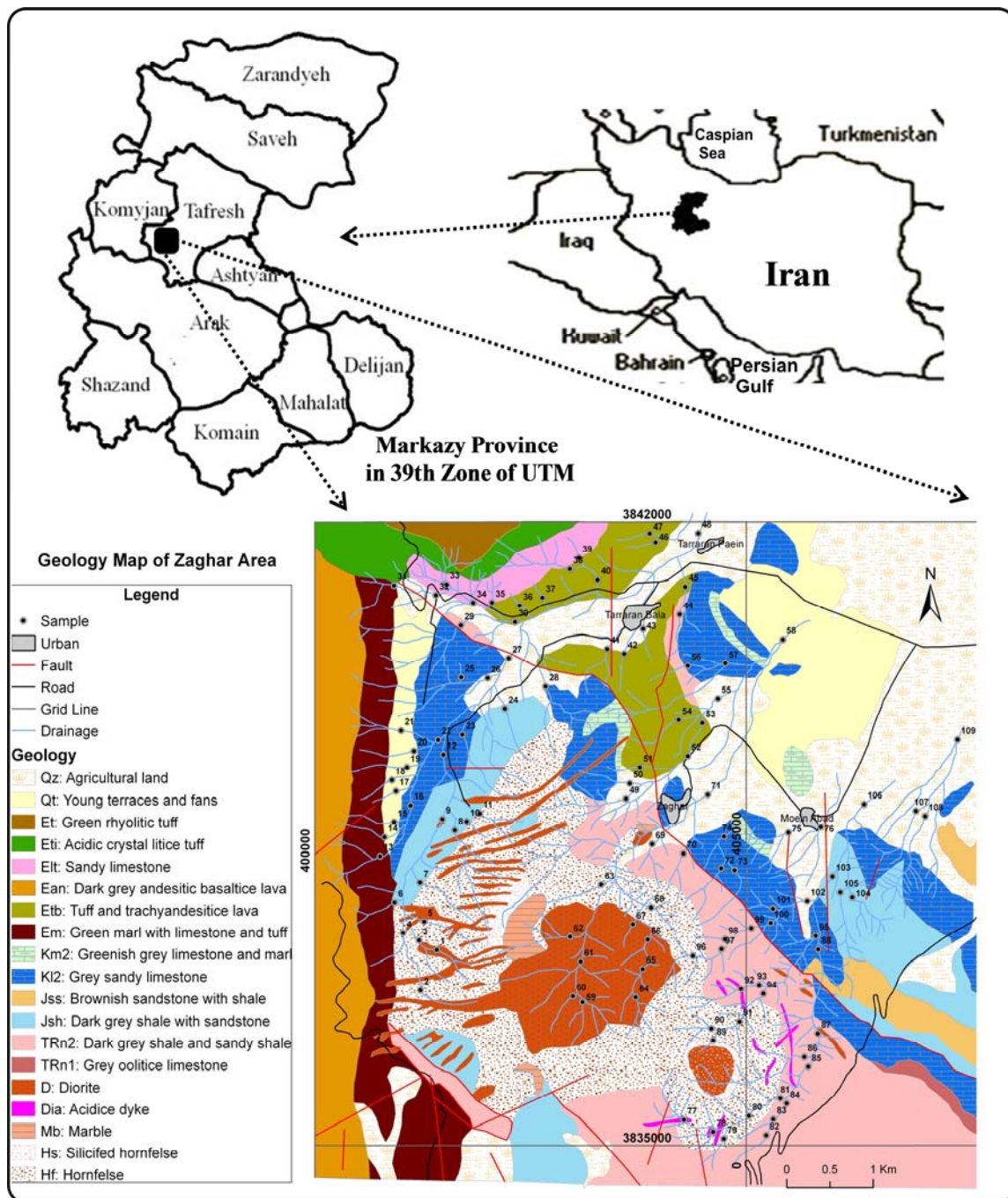


Figure 1. Location of study area in Iran and simplified geological map

These input sources have an inhomogeneous distribution within catchments and can be localized in circumscribed areas (point sources). Conversely, inputs rising from erosion/deposition processes are widespread in the catchments but act with different intensities according to the local geomorphologic and hydrological features.

The Extended Sample Catchment Basin (ESCB)

mapping technique, discussed in this paper, can be used to display the spatial distribution of geochemical variables measured in stream sediments taking into consideration the geomorphologic settings and the hydrographic patterns of surveyed areas (Spadoni *et al.*, 2005; Spadoni, 2006).

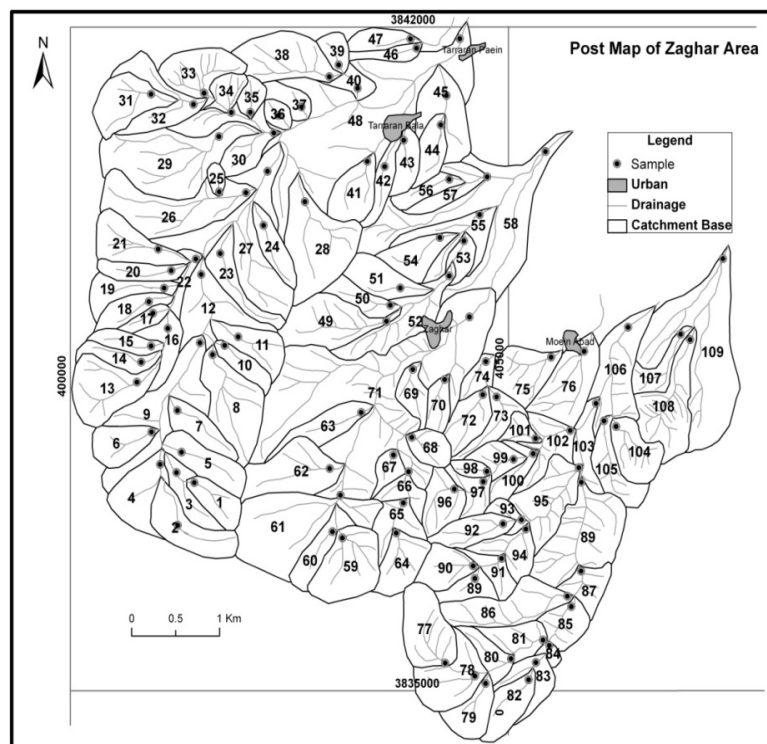


Figure 2. Use of ESCB technique in the Zaghar of Tafresh basin

This approach is based on the association of an area of statistical representativeness with each sample and on the assumption that the concentrations measured in the stream sediments can be considered as average reference values for this area. ESCBs can be easily identified considering the position of the sampling points within the hydrographic network and using the confluences between the streams of highest rank as break points for representing changes of the geochemical background.

Over a total basin surface of about 34.15 km², 109 stream sediment samples (150 µm particle size diameter) were collected with an average sampling density of 1 sample/0.31 km² (Fig. 2). The concentration of 9 chemical elements (Au, Cu, Pb, Zn, Ag, Mo, W, Sn, and As) was measured by ICP-MS and the analytical precision was between 1 and 3%. Afterwards, ESCB mapping were tested and compared using GIS functions of spatial analysis.

Data Transformation

A total of variables (Au, Cu, Pb, Zn, Ag, Mo, W, Sn, and As) from 109 stream sediment data were used in our analysis. Because these variables are not symmetrically distributed, we examined normality

of each variable based on skewness and, if a variable does not have normality, we transformed variables (Reimann & Filzmoser, 2000). In our data set, none of the variables passed this normality distribution (Fig. 3). Therefore, log ratio transformations were conducted for the skewed variables to achieve normality and transformation (Aitchison, 1986; Egozcue *et al.*, 2003; Carranza, 2011). In our work, the results of isometric log ratio (ilr) transformations were nearly similar, and therefore, we selected log transformation.

Multivariate Analysis

In order to determine relationships among the elements and the element groups stepwise factor analysis, correlation analysis and cluster analysis were employed. Results of the analyses were evaluated with STATISTICA 8.

The factor analysis was carried out with the principal component method which is, rather than the original data, based on the examination of dependency among the artificial variables which are computed from covariance and correlation coefficient matrixes (Jolliffe, 2002; Yousefi *et al.*, 2012).

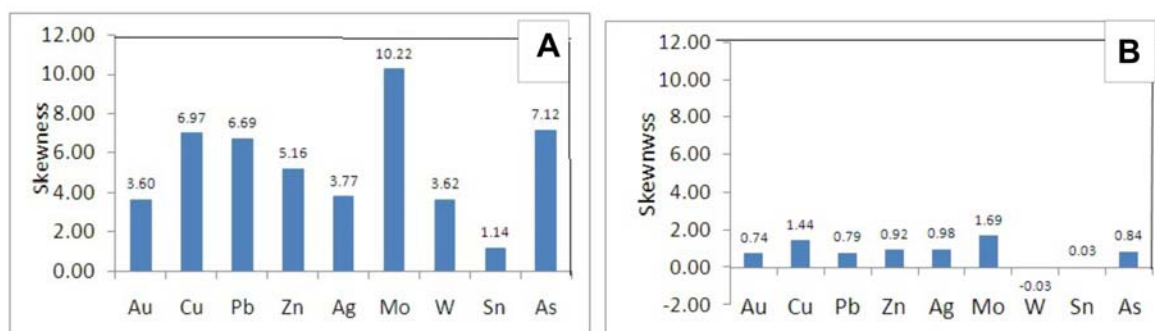


Figure 3. Comparison of skewness in (A) raw data and (B) log transformation data

In other words, eigenvalues and eigenvectors of covariance and correlation coefficient matrixes are interpreted. In the meantime, to strengthen the factor loads, varimax rotation was performed. Using Ward's method, Pearson's correlation coefficients cluster analysis (hierarchical cluster analysis) was carried out and the results are given in a dendrogram.

Fractal modeling

Fractal and multifractal are two important concepts in the fields of non-linear and complexity sciences and have been recognized in the geosciences (Cheng *et al.*, 1994). Fractal model is a powerful tool for identifying geochemical anomalies and/or determining geochemical baselines in various studies (Cheng *et al.*, 2010; Afzal *et al.*, 2011, 2013; Carranza, 2011; Arias *et al.*, 2012). Several models have been developed for geochemical data.

The concentration area (C-A) fractal model is one of the most important fractal models which is widely used in geochemical exploration. This model serves to illustrate the correlated relationship between the obtained results with the geological, geochemical, and mineralogical information. Its most useful features are its easy implementation and ability to compute quantitative anomalous thresholds. Cheng *et al.* (1994) proposed an element C-A fractal model which may be used to define the geochemical background and anomalies.

A sub-catchment map provides a smoothed version of the spatial distribution of an element. Sub-catchment maps were used to obtain approximate relations between areas $A(\rho)$ and concentration values ρ , with $A(\rho)$ decreasing for increasing ρ . Conversely, the area with concentration values less than ρ is an increasing function of ρ . If the element concentration per unit area satisfies a fractal or multifractal model, then the area $A(\rho)$ has indeed a power-law relation with

ρ . When the concentration per unit area follows a fractal model, this power-law relation has only one exponent. On the other hand, when the concentration per unit area satisfies a multifractal model with a spectrum of fractal dimensions, then several separate power-law relations between area $A(\rho)$ can be established. For a range of ρ close to its minimum value ρ , the predicted multifractal power-law relations are (Eq.1):

$$A(\rho \leq \nu) \propto \rho^{-a_1}; A(\rho > \nu) \propto \rho^{-a_2} \quad (1)$$

where $A(\rho)$ denotes the area with concentration values greater than the catchment value ρ ; ν represents the threshold; and a_1 and a_2 are characteristic exponents (Afzal *et al.*, 2010; Zuo, 2011). For most elements of interest, the area $A(\rho)$ as determined from sub-catchment maps generally has approximately two separate power-law relations with ρ over restricted ranges of ρ . Relationships between $A(\rho)$ and ρ on log-log plots for element which are of a different type. The breaks between straight-line segments on this plot and the corresponding values of ρ have been used as thresholds to separate geochemical values into different components, representing different causal factors, such as lithological differences and geochemical processes (Arias *et al.*, 2012; Geranian *et al.*, 2013). Factors such as mineralizing events, surficial geochemical element concentrations, and surficial weathering are of considerable importance.

This method has several limitation and accuracy problems, especially when the boundary effects on irregular geometrical data sets are involved. The C-A fractal model seems to be equally applicable as well to all cases, which is probably rooted in the fact that geochemical distributions mostly satisfy the properties of a multifractal function. Some approaches seem to support the idea that geochemical data distributions are multifractal, although this point is far from being proven (Geranian *et al.*, 2013). This idea may provide and

help the development of an alternative interpretation validation and useful methods to be applied to elemental geochemical distributions analysis.

Results and Discussion

Elemental concentrations of sediments

Descriptive statistics such as minimum, median, mean, maximum, and percentiles (25, and 75%) for nine elements used in this study are shown in Figure 4 and Table 1. Most of the elements have a wide range of variations of several magnitudes. The comparison of elements in stream sediments of the study area with the values of upper continental crust has shown that mean of all elements(except As) exhibits high relative to upper continental crust based on Rudnick and Gao (2003). Therefore, there are many stream sediments that show anomaly

values and are high relative to background.

Statistical analysis

We used the principal component analysis for extraction of factors. Furthermore, we applied varimax rotation of factors (Kaiser, 1958). Then, we used a two-step factor analysis to extract components representing anomalous multi-element geochemical signatures (Yousefi *et al.*, 2012).

In the first step, factor analysis yielded four rotated components, each with eigenvalues greater than 1 (Table 2). Nine elements were combined to produce four significant factors explaining 66.87% of the variance of the original data set (Table 2). Most of the variance in the original data set is contained in the factor 1 (22.12%), which is associated with the component W (Table 2).

Table 1. Statistical parameters of elemental concentrations of sediments

	Mean	Median	Minimum	Maximum	Lower quartile	Upper quartile	Skewness
Au	0.020	0.005	0.001	0.240	0.002	0.022	3.600
Cu	60.49	28.00	4.00	1380	17.00	45.00	7.00
Pb	20.55	12.00	2.00	320	7.00	20	7.00
Zn	92.84	75.00	30.00	715	55.00	95.00	5.00
Ag	0.16	0.14	0.08	0.80	0.12	0.18	3.80
Mo	7.45	2.40	0.52	400	1.40	4.40	10.00
W	2.70	2.19	0.30	20	1.13	3.14	3.61
Sn	4.81	4.30	2.00	12	3.30	6.00	1.13
As	2.09	1.00	0.30	46	0.50	1.97	7.00

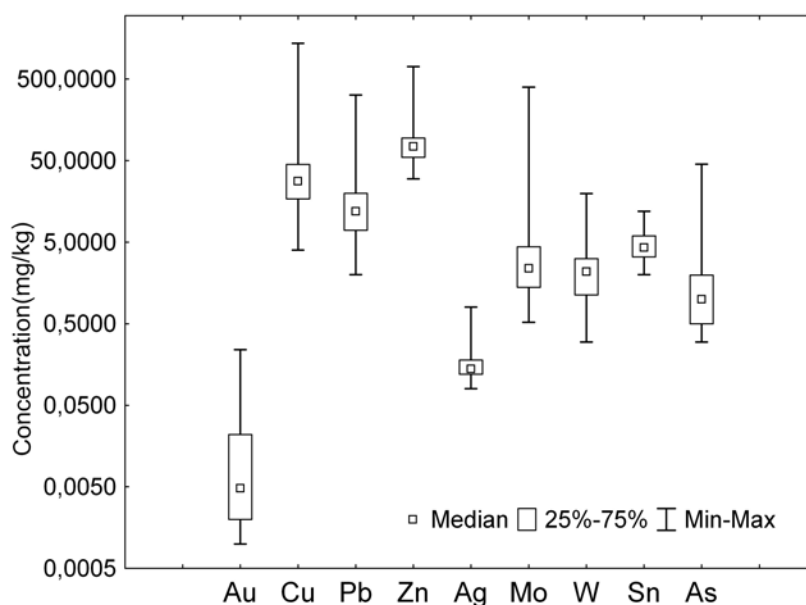


Figure 4. Elemental concentrations of sediments in Zaghar area

Factor 2 explains 19.87% of the variance and is mainly related to elements Pb and Ag. The Sn contributes most strongly to the third factor that explains 13.47% of the total variance. The fourth factor is concerned solely with Au and represents 11.40% of the total variance.

We can reduce the number of factors and increase the anomaly intensity using stepwise factor analysis. Increasing anomaly intensity means that the number of adjacent anomalous samples in

sediments has increased with respect to the total number of anomalous samples in the study area. In order to achieve this, the data for Cu, Zn, Mo, and As which have weak correlations were omitted in all factors. Then, results of the second factor analysis of the remaining geochemical data were used to calculate factor scores for each sample. The rotated factor matrix and the factor plot in rotated space for the second factor analysis are shown in Table 3 and Figure 5.

Table 2. Rotated factor analysis in first step (loadings in bold represent the selected factors based on threshold of 0.7)

	Factor 1	Factor 2	Factor 3	Factor 4
Au	0.09	-0.02	0.03	0.82
Cu	0.06	0.21	-0.54	0.42
Pb	-0.01	0.79	0.10	-0.25
Zn	-0.49	0.40	0.03	-0.49
Ag	0.07	0.83	0.01	0.18
Mo	0.59	0.32	-0.25	0.15
W	0.89	-0.08	0.16	0.02
Sn	0.10	0.08	0.74	0.02
As	-0.22	0.37	0.56	0.32
% Total - variance	22.12	19.87	13.47	11.40
Cumulative - %	22.12	42.00	55.46	66.87

Table 3. Rotated factor analysis in second step of factor analysis (loadings in bold represent the selected factors based on threshold of 0.7)

	Factor 1	Factor 2	Factor 3	Factor 4
Au	-0.01	0.01	0.98	0.07
Pb	0.86	-0.06	-0.16	0.05
Ag	0.84	0.14	0.16	-0.08
W	-0.01	0.09	0.07	0.98
Sn	0.05	0.98	0.01	0.09
% Total - variance	30.03	24.80	19.30	16.17
Cumulative - %	30.03	54.83	74.14	90.32

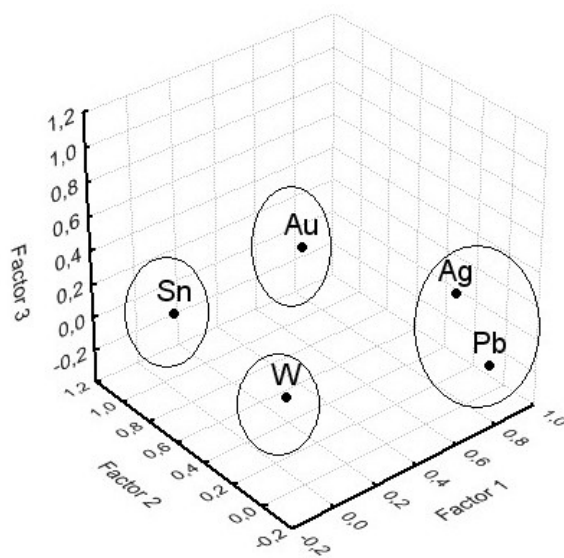


Figure 5. Factor plot in rotated space in second step of factor analysis

Factor 1 represents a Pb-Ag association, factor 2 is related to Sn, and factor 3 and factor 4 show Au and W, respectively.

According to Tables 2 and 3, the total variance relevant to the Pb-Ag association has increased from 19.87% in the first factor analysis to 30.03% in the second factor analysis. Likewise, the total variances relevant to the Sn and Au increased from 13.47% and 11.40% in the first factor analysis to 24.80% and 19.31% in the second factor analysis, respectively. But the total variances relevant to the W decreased from 22.12% in the first factor analysis to 16.18%. Consequently, through stepwise factor analysis, poor indicator elements are removed from the data and the total variance related to each factor has been increased.

In order to reveal relationship between elements and element groups in the second factor analysis, other multivariate analysis techniques such as cluster and correlation matrix analysis were performed. Using Ward's method and Pearson's correlation coefficients, cluster analysis (hierarchical cluster analysis) was carried out and the results are given in a dendrogram (Fig. 6). Results of cluster analysis indicate that the elements comprise two main groups. The first group is

composed of Ag and Pb. The second group is composed of three subgroups and consisting of Au, W and Sn. Both groups coincide with the results of factor analysis and correlation coefficients in correlation analysis (Table 4).

Factor analysis allows us to calculate a single value for each factor (Cheng *et al.*, 2011; Zao, 2011). For example, instead of analyzing separate element maps, we can establish a linear relationship among variables and plot a single map as called factor score map (FS) showing the distribution of such relationship (Yousefi *et al.*, 2012; 2013). Distribution maps of FS1 (Pb-Ag), FS2 (Sn), FS3 (Au), and FS4 (W) are represented as interpolated values (Fig. 7). Potential map was obtained by combining individual FS maps into a single geochemical predictive map and locations of the study area were selected as target areas for further exploration of the deposit-type. After the FSs of each sample, weights should be assigned to each sample to represent probability of the presence of the deposit-type upstream of the sample. The weights are here called the geochemical mineralization probability index map (GMPI: Zuo *et al.*, 2009a; Yousefi *et al.*, 2012).

Table 4. Pearson correlation coefficient matrix for elements in the sediments ($p \leq 0.01$)

	Au	Pb	Ag	W	Sn
Au	1				
Pb	-0.09	1			
Ag	0.07	0.47	1		
W	0.13	-0.02	-0.03	1	
Sn	0.03	0.03	0.12	0.17	1

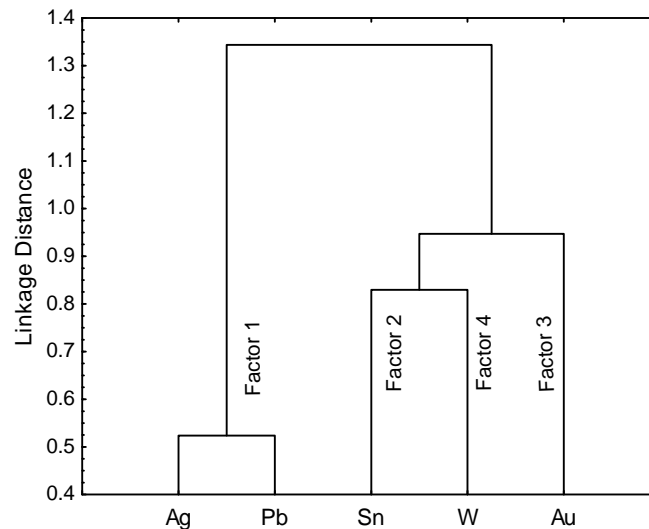


Figure 6. Dendrogram depicting the hierarchical clustering of the elements

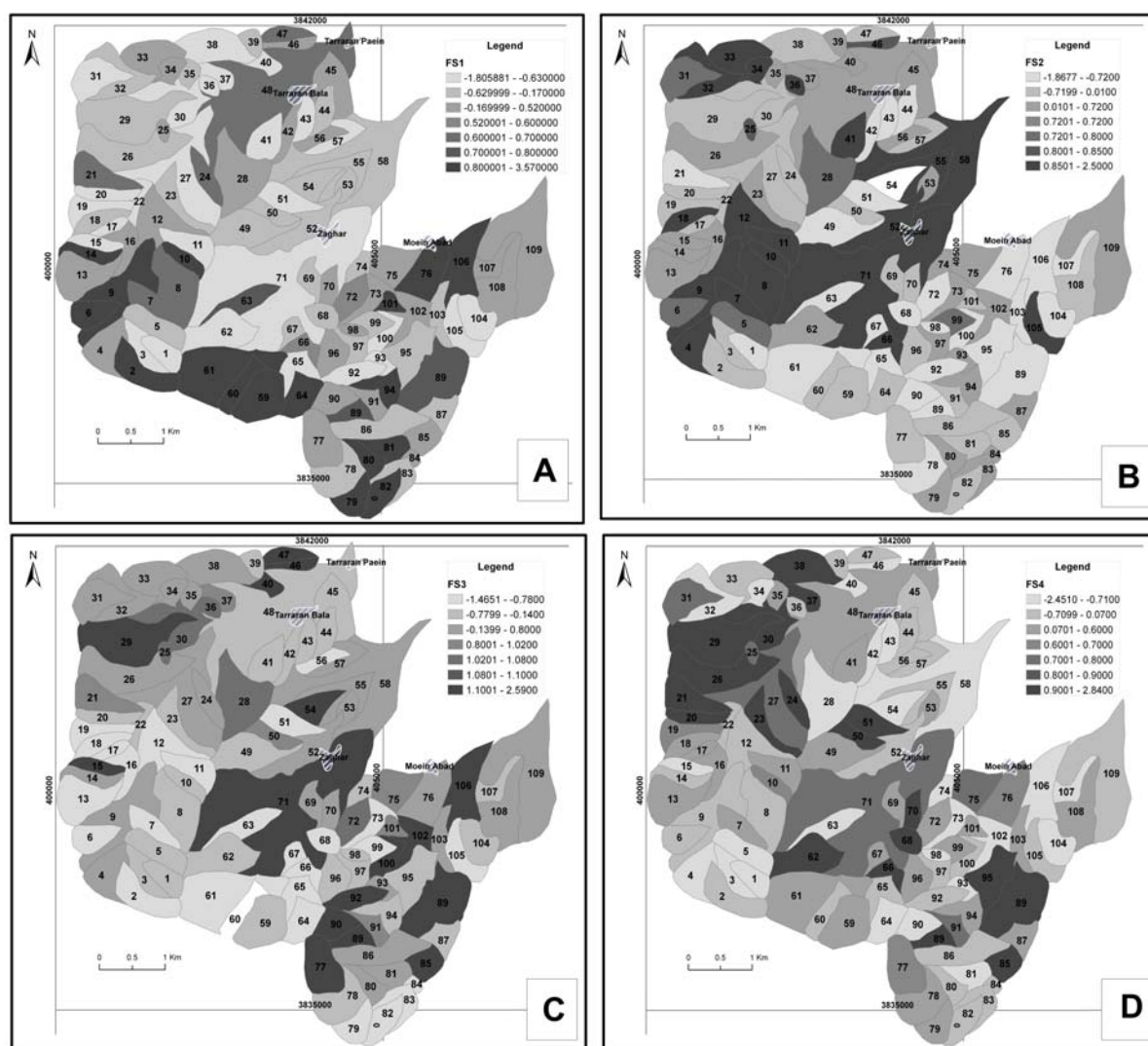


Figure 7. FS distribution map for (A) Pb-Ag(FS1); (B) Sn(FS2); (C) Au(FS3); and (D) W(FS4) indicator factor based on maximum, 99.5%, 97.5%, 84%, 75%, 50%, 25%, and minimum contents

In general factor analysis, the response variable is continuous and the values outside the [0, 1] range are inappropriate if the response variable relates to probability. In order to constrain the values of the predicted response variable within the unit interval [0,1], Yousefi *et al.* (2012,2013,2014) and Yousefi and Carranza (2015) recommended using a logistic model to represent the probability by Eq. (2).

$$GMPI = \frac{e^{MS}}{1 + e^{FS}} \quad (2)$$

where FS is the factor score of each sample per indicator factor obtained in a factor analysis. The GMPI is, therefore, a fuzzy weight of each stream sediment geochemical sample for each indicator factor. In this way, the weights of different classes of evidential maps are calculated based on the FSs

of samples per indicator factor obtained in the stepwise factor analysis. Values of the GMPI corresponding to cumulative content of maximum, 99.5%, 97.5%, 84%, 75%, 50%, 25%, and minimum were determined for the Pb-Ag, Sn, Au, and W indicator factors (Table 5) for mapping purposes.

In this study, the distributions of GMPI for indicator factors are represented as interpolated values (Fig. 8). A value of the GMPI corresponding to cumulative percentile of 97.5% frequency was selected as the threshold value to separate anomalous and background samples, like in the FS distribution maps (Fig. 7). The map of the first factor score (FS1) and geochemical mineralization probability index (GMPI: Figs. 7, 8, 1) shows high

values disposed in silicified hornfels related to dioritic intrusive, tuff, and trachy -andesitic lava in Eocene.

The first factor scores represent, however, mixed geochemical populations because the Urumieh-Dokhtar belt has a complex geological structure and different tectonic zones showing different

geochemical background ranges and thresholds. The second factor scores (FS2) and geochemical mineralization probability index (GMPI2) represent the high-frequency anomaly which is generally related to diorite intrusive and silicified hornfels which are favorable areas for Sn deposits.

Table 5. The FS and GMPI values corresponding to cumulative contents of maximum, 99.5%, 97.5%, 84%, 75%, 50%, 25% and minimum for Pb-Ag, Sn, Au and W indicator factors

	Factor Score(FS)				Geochemical mineralization probability index (GMPI)			
	FS1	FS2	FS3	FS4	GMPI1	GMPI2	GMPI3	GMPI4
Min	-1.81	-1.87	-1.46	-2.45	0.14	0.13	0.19	0.08
25%	-0.63	-0.72	-0.78	-0.71	0.35	0.33	0.31	0.33
50%	-0.17	0.01	-0.14	0.07	0.46	0.50	0.46	0.52
75%	0.52	0.72	0.80	0.60	0.63	0.67	0.69	0.65
84%	0.60	0.76	1.02	0.70	0.66	0.69	0.72	0.68
97.5%	0.70	0.80	1.08	0.80	0.67	0.70	0.73	0.70
99.5%	0.80	0.85	1.10	0.90	0.69	0.72	0.75	0.72
Max.	3.57	2.50	2.59	2.84	0.97	0.92	0.93	0.94

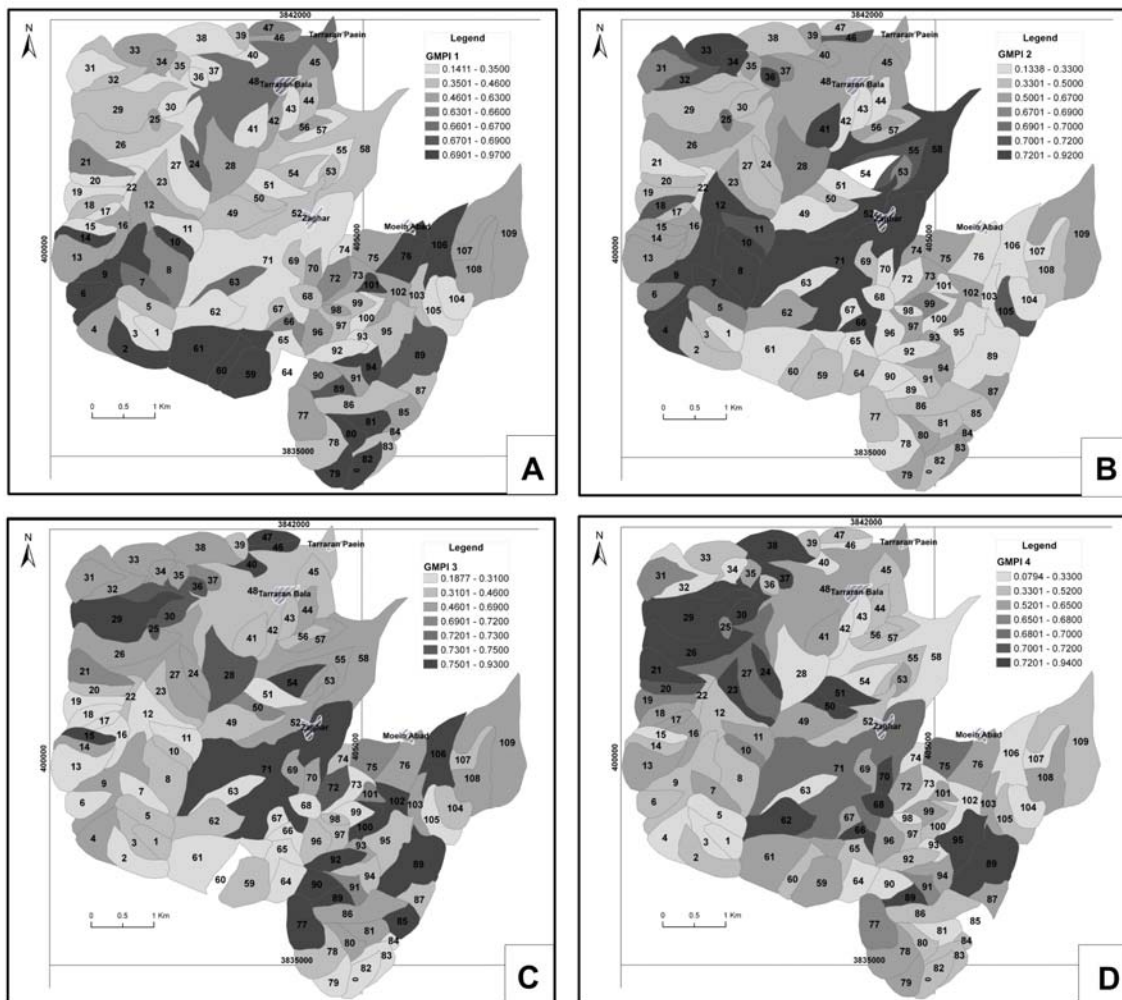


Figure 8. GMPI distribution map for (A) Pb-Ag(GMPI1); (B)Sn(GMPI2); (C) Au(GMPI3); and (D) W(GMPI4) indicator factor based on maximum, 99.5%, 97.5%, 84%, 75%, 50%, 25%, and minimum contents

The third factor scores (FS3) and geochemical mineralization probability index (GMPI3) map (Figs. 7, 8, 1) show that high values occur along Zaghar fault, or in the vicinity of fault intersections with Cretaceous limestone and in acidic dyke, which are favorable areas for Au skarn deposits. These results indicate potential for the discovery of Au skarn deposits in the study area. The fourth factor scores (FS4) and geochemical mineralization probability index (GMPI4) represent the high-frequency anomaly, which is generally related to marl with limestone, tuff, and andesitic, basaltic lava in Eocene which are favorable zones for W deposits.

Separation of anomaly and background using multifractal modeling

The area was divided to 109 sub-catchments. The proposed sub-catchments pattern is put to use

because the fundamentals of C-A fractal model is based on the existence of partition function. The necessary and the needed partition function to be used in fractal models is based upon assumption of having a catchment characterization in the area in order to find and calculate the area which has a certain ore grade (Cheng *et al.*, 1994; Spadoni *et al.*, 2005). The C-A relations were computed by assigning an area of influence to each sampled point and summing all elemental areas whose concentration lies below a given value. This procedure was repeated for different elemental concentrations (Zuo & Xia, 2009; Carranza, 2010; Afzal *et al.*, 2010, 2013; Arias *et al.*, 2012; Geranian *et al.*, 2013; Soltani *et al.*, 2014). The evaluated grades in catchments were sorted out based on decreasing grades and cumulative areas were calculated for grades (Cheng *et al.*, 1994).

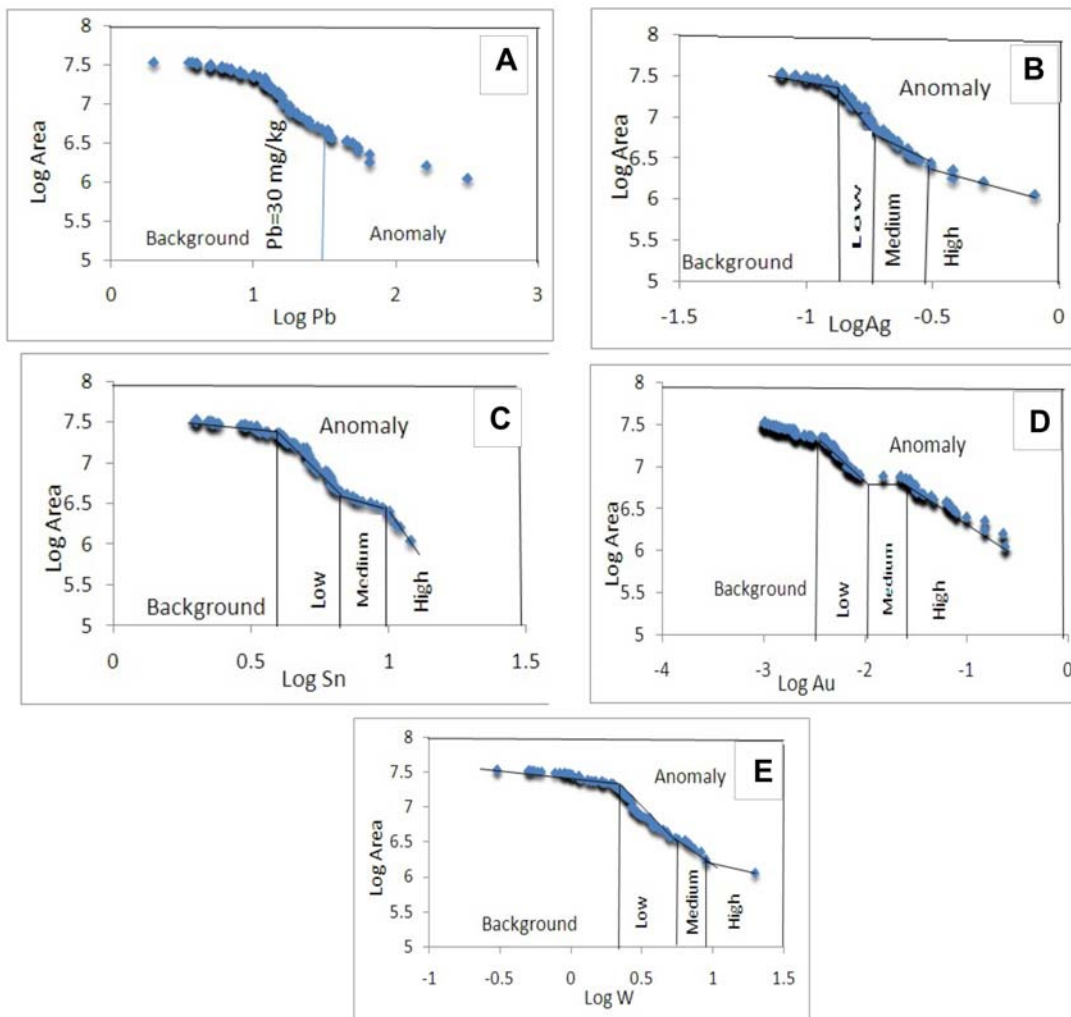


Figure 9. C-A log plots for (A) Pb;(B)Ag; (C)Sn;(D) Au; and (E) W component

The C-A fractal model was applied to decompose the mixed geochemical populations and identify geochemical anomalies in all component scores. Finally, log-log plots were constructed for Pb, Ag, Sn, Au, and W (Fig. 9).

Generally, the number of straight lines to be fitted to the data using the least squares method can be determined in terms of (1) how good the fitting will be, (2) how significant the difference between the slopes of straight lines fitted to the data will be, and (3) whether the results can be geologically interpreted (Arias *et al.*, 2012).

In this study, the C-A fractal plot can be fitted either with four straight lines (four-line model), or single straight line (one-line model). The regression errors for four-line model are lower than those of one-line model, indicating that the four-line model is better than one-line model. Four-line model is applied to fit the C-A fractal plot (Fig. 9). The right-hand lines represent the low, medium, and high-frequency anomaly and the left-hand line represents the low-frequency background component which may be related to favorable rock types (Arias *et al.*, 2012).

On the basis of this procedure, there are several populations for Pb, Ag, Sn, Au, and W respectively as shown in Figure 9, but we selected the best population. Lead anomalous threshold is 52 mg/kg based on log-log plot as depicted in Figure 9. Silver log-log plot shows that major Ag enrichment occurred at 0.25 mg/kg. Tin anomalous threshold is about 9.0 mg/kg. Major Au enrichment started from 0.0251 mg/kg, and for W is 6.2 mg/kg. Break between the straight-line segment and the corresponding values of Pb, Ag, Sn, Au, and W have been used as cut-offs to reclassify catchment values in the interpolated maps (Geranian *et al.*, 2013).

The main maps are indicated in Figure 10. Interpolated maps of the distribution of Pb, Ag, Sn, Au, and W, based on the modeled populations by the values equal to maximum, 99.5%, 97.5%, 84%, 75%, 50%, 25%, and minimum cumulative contents are presented in Figure 10. A final main map value corresponding to 97.5% cumulative percentile is used to generate the final distribution map for comparison with the multifractal maps obtained from fractal model (Fig. 11). The 97.5% cumulative percentile has been considered in all distribution maps for comparison purposes. The anomaly map (Fig. 11) shows that high values of Au follow an

NE–SW trend and occur around mapped intrusions close to limestone in northern part of the study area and along NE–SW trending dykes or in the vicinity of fault intersections, which are favorable areas for Au skarn deposits.

Figures 10 and 11 show the target areas for Au delineated by means of Au concentration values and fractal model. Target areas delineated based on concentration values and fractal model is mainly located in the NE-SW part of the study area. The most favorable areas for occurrence of Au deposits are mainly located in the SW which has been classified as skarn deposit area since more than 5 Au deposits have already been discovered in it, whereas no Au deposits have been discovered in other areas. The Au anomalies in other areas probably mainly reflect higher background values. The C-A fractal model proposed by Cheng *et al.* (1994) was used for separation of anomalies from background.

Figure 9 shows the log-log plots of Au values versus area for the whole study area. Figure 11 shows the target areas for Au delineated on the basis of $Au \geq 0.0030$ mg/kg, $Au \geq 0.0060$ mg/kg, and $Au \geq 0.0251$ mg/kg for the whole study area. Comparing different methods such as factor score (FS-Au), geochemical mineralization probability index (GMPI -Au), main concentration (Au), and fractal model (Fr-Au) in Figure 12, the main difference is the area occupied by Au deposits. The targets in Figure 12 are nearly similar, indicating that the fractal model and other methods could clearly identify high anomalies for the study area. However, the target areas for Au deposits in fractal model (Fr-Au) are like those in main concentration (Au) in the study area.

The anomaly map (Fig. 12) shows that high values of Au follow an NW–SE trend and occur around mapped intrusions and along NW–SE trending faults or in the vicinity of fault intersections, which are favorable areas for skarn deposits. These results indicate potential for discovery of Au skarn deposits in the study area. The integrated anomalies of Pb, Ag, Sn, and W occurring around the intrusions and in the vicinity of faults in the center part of the study area should be further investigated in the next step of mineral resource exploration. However, the anomalies occurring in southern part of the study area may be caused by high background concentration values of bed rocks.

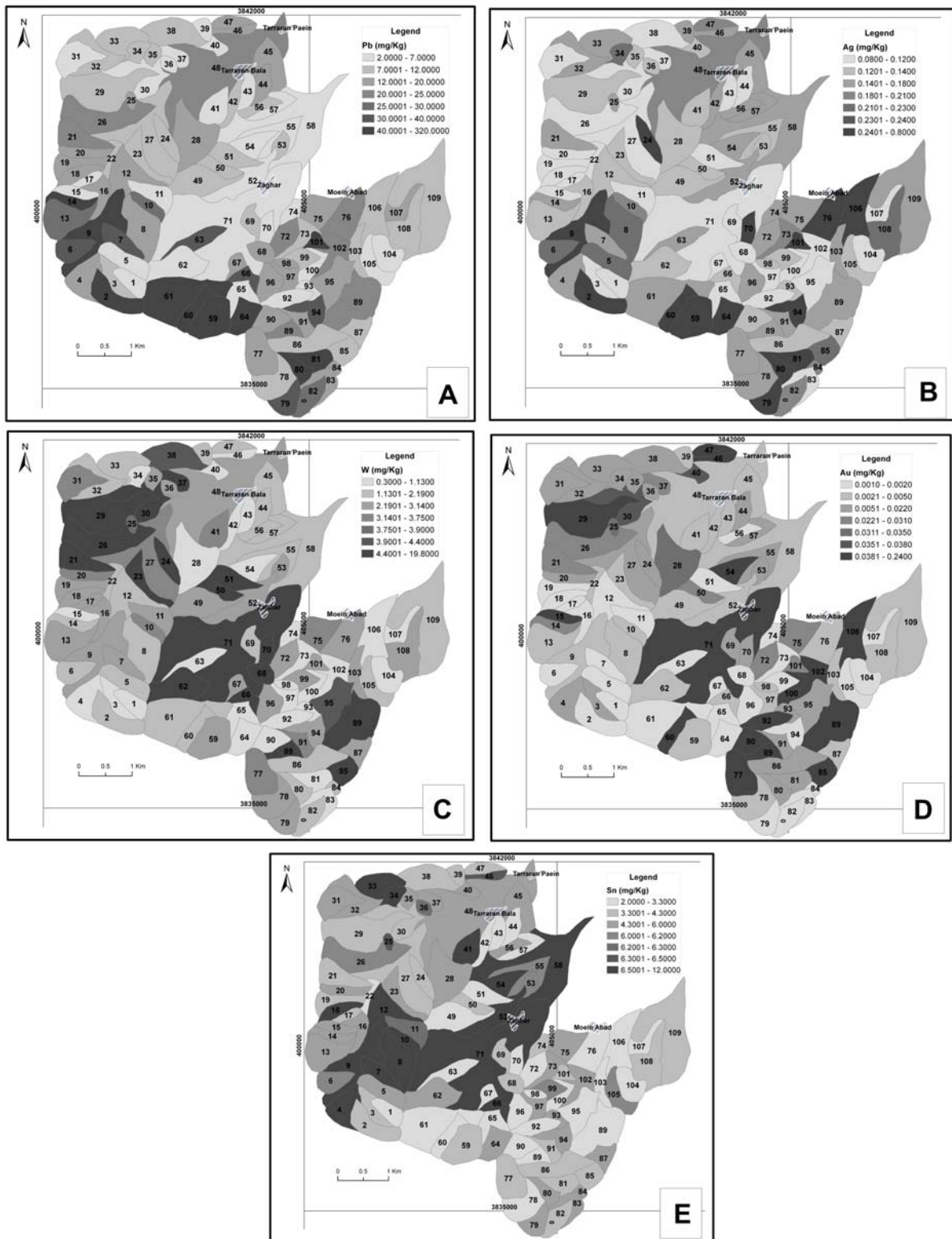


Figure 10. Distribution map of (A) Pb, (B) Ag, (C) W, (D) Au; and (E) Sn, plotted based on maximum, 99.5%, 97.5%, 84%, 75%, 50%, 25%, and minimum contents

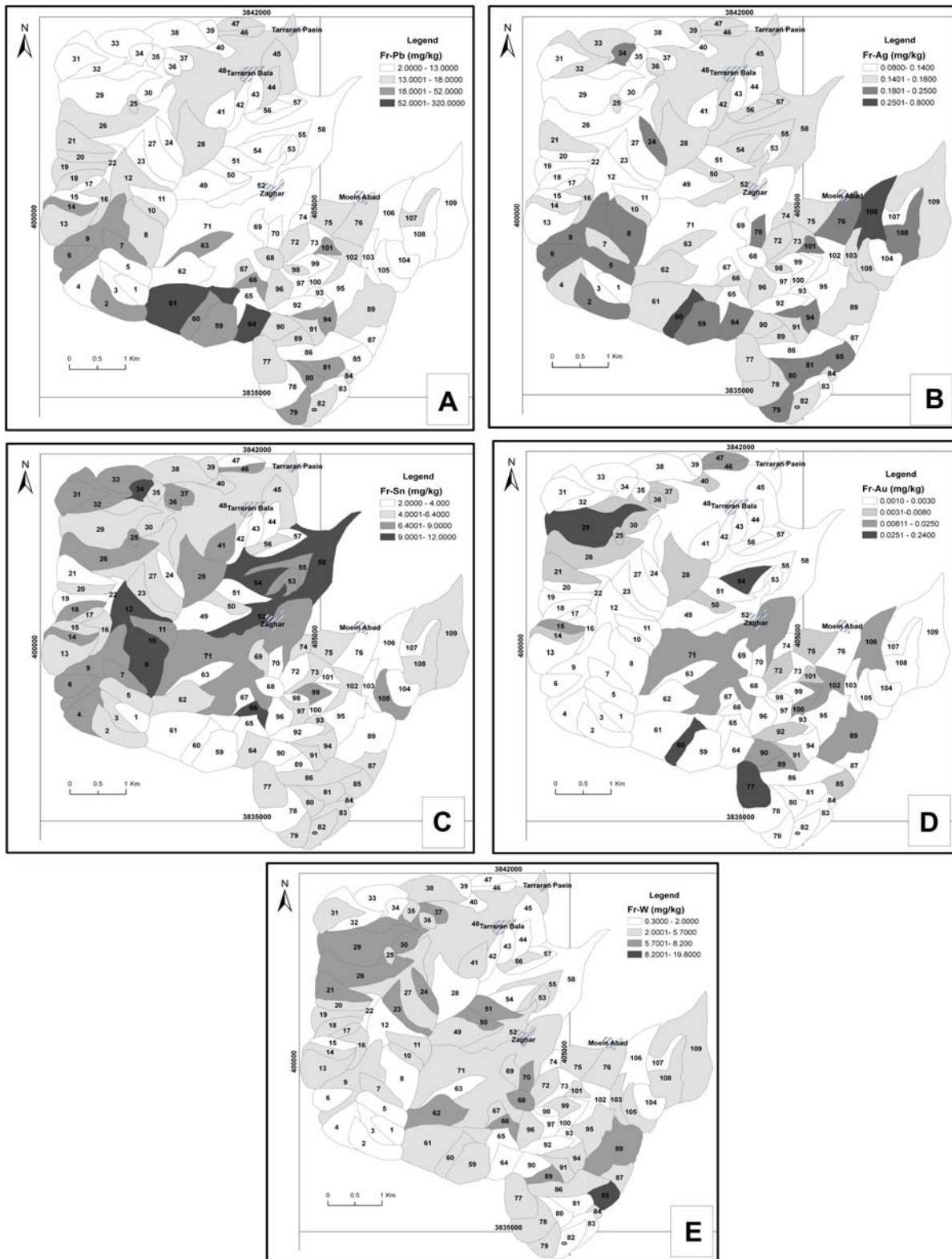


Figure 11. Distribution map of(A) Pb,(B)Ag,(C) Sn, (D)Au; and (E)W, plotted based on threshold of fractal method

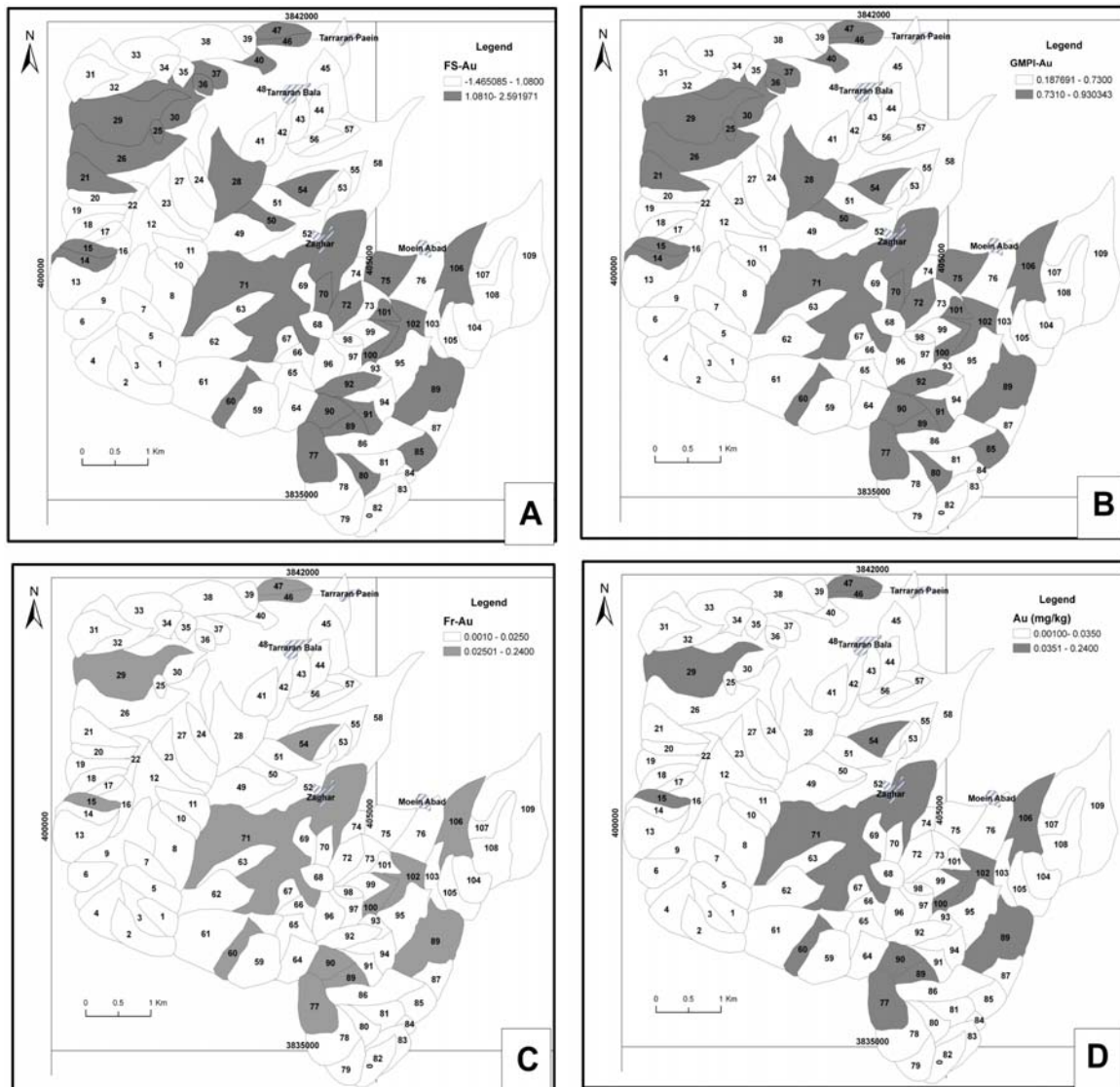


Figure 12. Targets delineated by means of factor score A) (FS-Au), B) geochemical mineralization probability index (GMPI -Au), C) fractal method (Fr-Au), and D) main concentration (Au)

Conclusions

This study suggests that the Urumieh-Dokhtar Belt in Zaghar region of Tafrash city has great potential for skarn-type deposits. In this study, the statistical analysis and C-A fractal model were used to identify geochemical anomalies associated with Au skarn mineralization. The following conclusions are obtained:

- Non-indicator factors and elements are recognized through stepwise factor analysis and cluster analysis.
- Stepwise factor analysis increases the percentage of total explained data variance by removal of non-indicator elements.
- Anomaly intensity, especially around known

dioritic intrusions, is enhanced in the FS and GMPI anomaly maps.

-The target Au map area indicates that the fractal model along with other methods represent similar trend for high anomalies of Au deposits.

- The anomaly map shows that Au deposits occur around intrusions and along dykes or in the vicinity of fault intersections with the Cretaceous limestone which are favorable areas for Au skarn prospectivity.

-The integrated anomalies of Pb-Ag, Sn, Au, and W occurring around the intrusions and in the vicinity of dykes should be further investigated in the next phase of mineral exploration.

Acknowledgments

The authors thank Mining Organization of Markazi Province for the results of elemental data. We also

appreciate the comments of the anonymous reviewers.

References

- Afzal, P., Khakzad, A., Moarefvand, P., Rashidnejad, N.O., Esfandiari, B., FadakarAlghalandis, Y., 2010. Geochemical anomaly separation by multifractal modeling inKahang (GorGor) porphyry system, Central Iran .Journal of Geochemical Exploration 104, 34–46.
- Afzal, P., FadakarAlghalandis, Y., Khakzad, A., Moarefvand, P., RashidnejadOmran, N., 2011. Delineation of mineralization zones in porphyry Cu deposits by fractal concentration–volume modeling, Journal of Geochemical Exploration 108, 220–232.
- Afzal, P., Harati, H., FadakarAlghalandis, Y., Yasrebi, A.B., 2013. Application of spectrum–area fractal model to identify of geochemical anomalies based on soil data in Kahang porphyry-type Cu deposit, Iran, Chemie der Erde - Geochemistry, Volume 73, Issue 4, December 2013, 533-543.
- Afzal, P., Alhoseini, S.H., Tokhmechi, B., KavehAhangarana, D., Yasrebi, A.B., Madani, N., Wetherelt, A., 2014. Outlining of high quality coking coal by Concentration-Volume fractal Model and Turning Bands Simulation in East-Parvadeh Coal Deposit, Central Iran. International Journal of Coal Geology 127: 88-99.
- Aitchison, J., 1986. The statistical analysis of compositional data. London, UK: Chapman and Hall; p. 416.
- Alavi, M., 1994. Tectonic of Zagros orogenic belt of Iran: new data and interpretations. Tectonophysics 229, 211–238.
- Arias, M., Gumiel, P., Marti-Izard, C., 2012. Multifractal analysis of geochemical anomalies: a tool for assessing prospectivity at the SE border of the Ossa Morena Zone, Variscan Massif (Spain). Journal of Geochemical Exploration 122, 101–112.
- Borna, B., 2004. Exploration studies of Au in TafrashZaghar, Geological Organization of Iran.
- Carranza E.J.M. 2009. Mapping of anomalies in continuous and discrete fields of stream sediment geochemical landscapes. Geochemistry: Exploration, Environment, Analysis. 10: 171–187.
- Carranza, E.J.M., 2010. Catchment basin modeling of stream sediment anomalies revisited: incorporation of EDA and fractal analysis. Geochemistry: Exploration, Environment, Analysis. 10: 365–381.
- Carranza, E.J.M., 2011. Analysis and mapping of geochemical anomalies using logratio-transformed stream sediment data with censored values. Journal of Geochemical Exploration. 110: 167–185.
- Cheng, Q., Agterberg, F.P., Ballantyne, S.B., 1994. The separation of geochemical anomalies from background by fractal methods. Journal of Geochemical Exploration. 54: 109–130.
- Cheng, Q., 2007. Mapping singularities with stream sediment geochemical data for prediction of undiscovered mineral deposits in Gejiu, Yunnan Province, China. Ore Geology Reviews. 32: 314–324.
- Cheng, Q., Agterberg, F.P., 2009. Singularity analysis of ore-mineral and toxic trace elements in stream sediments. Computers and Geosciences. 35: 234–244.
- Cheng, Q., Xia, Q., Li, W., Zhang, S., Chen, Z., Zuo, R., Wang, W., 2010. Density/area power–law models for separating multi-scale anomalies of ore and toxic elements in stream sediments in Gejiu mineral district, Yunnan Province, China. Biogeosciences. 7: 3019–3025.
- Cheng, Q., Bonham-Carter, G.F., Wang, W., Zhang, S., Li, W., Xia, Q., 2011. A spatially weighted principal component analysis for multi-element geochemical data for mapping locations of felsic intrusions in the Gejiu mineral district of Yunnan, China. Computers and Geosciences. 5: 662–669.
- Egozcue, J.J., Pawlowsky-Glahn, V., Mateu-Figueras, G., Barceló-Vidal, C., 2003. Isometric logratio transformations for compositional data analysis. Mathematical Geology. 35: 279- 300.
- Geranian, H., Mokhtari, A.R., Cohen,D.R., 2013. A comparison of fractal methods and probability plots in identifying and mapping soil metal contamination near an active mining area, Iran, Science of the Total Environment, 463-464.
- Grunsky E.C., Drew, L.J., and Sutphin, D.M., 2009. Process recognition in multi-element soil and stream-sediment geochemical data. Applied Geochemistry 24, 1602–1616.
- Grunsky, E.C., 2010. The interpretation of geochemical survey data. Geochemistry: Exploration, Environment, Analysis. 10: 27–74.
- Hajian, J., 1999. Geological map of Tafrash, Geological Organization of Iran.
- Heidari, M., Ghaderi, M., Afzal, P., 2013. Delineating mineralized phases based on litho-geochemical data using multifractal model in Touzlar epithermal Au-Ag (Cu) deposit, NW Iran. Applied Geochemistry. 31: 119-132.
- Jolliffe, T., 2002. Principal Component Analysis. Springer Verlag, New York.
- Johnson, R.A., Wichern, D.W., 2002. Applied Multivariate Statistical Analysis, 5th ed. Prentice Hall, Upper Saddle River, New Jersey.
- Kaiser, H.F., 1958. The varimax criterion for analytic rotation in factor analysis. Psychometrika. 23: 187-200.

- Lahermo, P., Väänänen, P., Tavainen, T., Salminen, R., 1996. Geochemical Atlas of Finland: Part 3. Environmental Geochemistry– Stream Waters and Sediments. Geological Survey of Finland, Espoo.
- Reimann, C., Filzmoser, P., 2000. Normal and lognormal data distribution in geochemistry: death of a myth. Consequences for the statistical treatment of geochemical and environmental data. *Environmental Geology*. 39: 1001–1014.
- Rudnick, R.L., Gao, S., 2003. Composition of the Continental Crust. In: Holland, H.D., Turekian, K.K. (eds-in-chief), *Treatise on Geochemistry Volume 3: Rudnick, R.L. (ed.), The Crust*, 1–64. Elsevier-Pergamon, Oxford.
- Salminen, R., Tarvainen, T., Demetriades, A., Duris, M., Fordyce, F. M., Gregorauskiene, V., Kahelin, H., Kivisilla, J., Klaver, G., Klein, H., Larson, J.O., Lis, J., Locutura, J., Marsina, K., Mjartanova, H., Mouvet, C., O'Connor, P., Odor L., Ottonello, G., Paukola, T., Plant, J.A., Reimann, C., Schermann, O., Siewers, U., Steenfelt, A., Van der Sluys, J., De Vivo, B., Williams, L., 1998. FOREGS geochemical mapping field manual. Geological Survey of Finland, p. 47.
- Shahabpour, J., 1994. Post-mineral breccia dyke from the Sar-Cheshmeh porphyry copper deposit, Kerman, Iran. *Exploration and Mining Geology*. 3: 39–43.
- Soltani, F., Afzal, P., Asghari, O., 2014. Delineation of alteration zones based on Sequential Gaussian Simulation and concentration–volume fractal modeling in the hypogene zone of Sungun copper deposit, NW Iran, *Journal of Geochemical Exploration*. 140: 64–76.
- Spadoni, M., Voltaggio, M., Cavarretta, G., 2005. Recognition of areas of anomalous concentration of potentially hazardous elements by means of a subcatchment-based discriminant analysis of stream sediments. *Journal of Geochemical Exploration*. 87: 83–91.
- Spadoni, M., 2006. Geochemical mapping using a geomorphologic approach based on catchments, *Journal of Geochemical Exploration*. 90: 183–196.
- Sun, X., Deng, J., Gong, Q., Wang, Q., Yang, L., Zhao, Z., 2009. Kohonen neural network and factor analysis based approach to geochemical data pattern recognition. *Journal of Geochemical Exploration*. 103: 6–16.
- Yousefi, M., Nykänen, V., 2015. Data-driven logistic-based weighting of geochemical and geological evidence layers in mineral prospectivity mapping, *Journal of Geochemical Exploration*, doi:10.1016/J.gexplo.2015.08.008.
- Yousefi, M., Carranza, E.J.M., 2015. Prediction–area (P–A) plot and C–A fractal analysis to classify and evaluate evidential maps for mineral prospectivity modeling, *Computers & Geosciences*. 79: 69–81.
- Yousefi, M., Carranza, E.J.M., 2014. Fuzzification of continuous-value spatial evidence for mineral prospectivity mapping. *Computer and Geoscience*. 74: 97–109.
- Yousefi, M., Kamkar-Rouhani, A., Carranza, E.J.M., 2014. Application of staged factor analysis and logistic function to create a fuzzy stream sediment geochemical evidence layer for mineral prospectivity mapping, *Geochemistry: Exploration, Environment, Analysis*. 14 (1): 45–58.
- Yousefi, M., Carranza, E.J.M., Kamkar-Rouhani, A., 2013. Weighted drainage catchment basin mapping of geochemical anomalies using stream sediment data for mineral potential modeling. *Journal of Geochemical Exploration*. 128: 88–96.
- Yousefi, M., Kamkar-Rouhani, A., Carranza, E.J.M., 2012. Geochemical mineralization probability index (GMPI): A new approach to generate enhanced stream sediment geochemical evidential map for increasing probability of success in mineral potential mapping. *Journal of Geochemical Exploration*. 115: 24–35.
- Zheng, Y., Sun, X., Gao, S., Wang, C., Zhao, Z., Song, J., 2014. Analysis of stream sediment data for exploring the Zhunuo porphyry Cu deposit, southern Tibet, *Journal of Geochemical Exploration*. Available online 1 March 2014.
- Zuo, R., Cheng, Q., Agterberg, F.P., 2009a. Application of a hybrid method combining multilevel fuzzy comprehensive evaluation with asymmetric fuzzy relation analysis to mapping prospectivity. *Ore Geology Reviews*. 35: 101–108.
- Zuo, R., Cheng, Q., Agterberg, F.P., Xia, Q., 2009b. Application of singularity mapping technique to identification local anomalies using stream sediment geochemical data, a case study from Gangdese, Tibet, Western China. *Journal of Geochemical Exploration*. 101: 225–235.
- Zuo, R., Xia, Q., 2009. Application fractal and multifractal methods to mapping prospectivity for metamorphosed sedimentary iron deposits using stream sediment geochemical data in eastern Hebei province, China. *Geochimica et Cosmochimica Acta*. 73: A1540–A1540.
- Zuo, R., 2011a. Decomposing of mixed pattern of arsenic using fractal model in Gangdese Belt, Tibet, China. *Applied Geochemistry*. 26: S271–S273.
- Zuo, R., Xia, Q., 2009. Application fractal and multifractal methods to mapping prospectivity for metamorphosed sedimentary iron deposits using stream sediment geochemical data in eastern Hebei province, China. *Geochimica et Cosmochimica Acta*. 73 A1540–A1540.
- Zuo, R., 2011. Identifying geochemical anomalies associated with Cu and Pb–Zn skarn mineralization using principal component analysis and spectrum-area fractal modeling in the Gandese Belt, Tibet (China). *J Geochem Explor*. 111: 13–22.
- Zuo, R., 2014. Identification of weak geochemical anomalies using robust neighborhood statistics coupled with GIS in covered areas, *Journal of Geochemical Exploration*, Volume 136, January. 2014: 93–101.